Available online at www.sciencedirect.com
SCIENCE DIRECT®
Journal of Contaminant Hydrology 72 (2004) 23–46
JOURNAL OF Contaminant Hydrology
www.elsevier.com/locate/jconhyd

Anomalous transport of colloids and solutes in a shear zone

Georg Kosakowski*

Paul Scherrer Institut, Nuclear Energy and Safety Research Department, Waste Management Laboratory, 5232 Villigen PSI, Switzerland

Received 20 May 2003; received in revised form 13 October 2003; accepted 31 October 2003

Abstract

Transport experiments with colloids and radionuclides in a shear zone were conducted during the Colloid and Radionuclide Retardation experiment (CRR) at Nagra's Grimsel Test Site. Breakthrough curves of bentonite colloids and uranine, a non-sorbing solute, were measured in an asymmetric dipole flow field. The colloid breakthrough is earlier than that of uranine. Both breakthrough curves show anomalously long late time tails and the slope of the late time tails for the colloids is slightly higher. Anomalous late time tails are commonly associated with matrix diffusion processes; the diffusive interaction of solutes transported in open channels with the adjacent porous rock matrix or zones of stagnant water. The breakthrough curves for different colloid size classes are very similar and show no signs of fractionation due to their (size-dependent) diffusivity. It is proposed that tailing of the colloids is mainly caused by the structure of the flow field and that for the colloid transport, matrix diffusion is of minor importance. This has consequences for the interpretation of the uranine breakthrough. Comparisons of experimental results with numerical studies and with the evaluation of the colloid breakthrough with continuous time random theory imply that the tailing in the conservative solute breakthrough in this shear zone is not only caused by matrix diffusion. Part of the tailing can be attributed to advective transport in fracture networks and advection in low velocity regions. Models based on the advection–dispersion equation and matrix diffusion do not properly describe the temporal and spatial evolution of colloid and solute transport in such systems with a consistent set of parameters.

Keywords: Fractured rock; Tracer test; Colloid transport; Matrix diffusion

* Fax: +41-56-310-28-21.
E-mail address: georg.kosakowski@psi.ch (G. Kosakowski).

0169-7722/$ - see front matter © 2003 Elsevier B.V. All rights reserved.
doi:10.1016/j.jconhyd.2003.10.005

1. Introduction

Robust models for the transport of solutes and colloidal particles in geological formations are of great interest in many fields, e.g. for the safety assessment of repositories for radioactive waste. A key problem is how to describe the movement of solutes and colloids in fractured and highly heterogeneous porous systems. Controlling factors for the case of fractured systems include the highly complex structure of the flow field due to variable fracture network geometry, small and large-scale roughness of the fracture walls, the presence of fracture filling material and interaction of the solutes and colloids with the rock matrix.

In Switzerland, the joint Nagra (Swiss National Cooperative for the Disposal of Radioactive Waste), PNC (Power Reactor and Nuclear Fuel Development Corporation, Japan) and PSI (Paul Scherrer Institut, Switzerland) Radionuclide Migration Programme began testing radionuclide transport models at Nagra's Grimsel Test Site more than 15 years ago under conditions as relevant as possible to the long-term evolution of geological repositories.

Earlier experiments (Migration Experiment, MI) concentrated on basic investigations and the characterization of the transport of non-sorbing and sorbing solutes in a shear zone in the granodioritic rock (McKinley et al., 1988; Frick et al., 1992; Smith et al., 2001; Ota et al., 2002). Hadermann and Heer (1996) evaluated dipole tracer experiments and found that they could describe the transport of solutes with a double porosity model. In their model approach, they represented the shear zone as a set of parallel open fractures embedded in a highly porous rock matrix (fault gouge) of finite extent. By considering advection, dispersion in the fractures, diffusion from the fractures perpendicularly into the rock matrix and sorption on the rock matrix, they could fit the breakthrough curves with material parameters consistent with independent information and make acceptable predictions for a different transport distance. They found that dispersion shows no dependency on the type of tracer used.

More recently, Nagra and JNC (Japan Nuclear-Cycle Research Institute) the successor to PNC, began the Excavation Experiment (EP), described in detail in Möri (2001), which focused on the detailed investigation of the structure of the shear zone. Tracer breakthrough curves were recorded in the same way as in the MI experiment. The tracer experiments were stopped before all of the injected radionuclides were completely recovered and a specially developed resin was injected into the shear zone to stabilize the rock and prevent disturbance of the in situ radionuclide distribution. Subsequently, the flow field was excavated with a triple-barrel drilling technique. The core analysis resulted in a 3D representation of the small-scale fracture network in the shear zone and its properties. In addition, the distribution of the retarded radionuclides was analyzed and it was found that the recovery of the remaining radionuclides in the excavated core was more than 90%. Although it was known that the shear zone is highly heterogeneous, the main result of the core analyses was that within the shear zone, open channels control the water flow to a very high degree. Further, it was verified that matrix pores are accessible to dissolved species because most of the retarded radionuclides were found in the highly porous fault gouge separating the open flow channels in the shear zone (Möri, 2001).

The current investigations form part of the Colloid and Radionuclide Retardation (CRR) project and focus on the influence of bentonite colloids on the radionuclide transport in the shear zone (Möri, in press). The breakthrough of the colloids shows unusually long late time tails, similar to those of solutes already investigated during the MI experiment. For the solutes, it was assumed that hydrodynamic dispersion can be described with a diffusion-like process obeying Ficks's law and that the tailing is caused by diffusion into a porous matrix. It will be shown in Section 5 of this paper that the colloids, in contrast to the solutes, do not undergo matrix diffusion. With the new data from the colloid breakthrough, it is then possible to test the hypothesis of Fickian dispersion.

Scale-dependent spreading of contaminant plumes, characterized by unusually early breakthrough times or unusually long late time tails in measured breakthrough curves, is often described in the frame of non-Fickian transport (e.g. Hatano and Hatano, 1998; Sidle et al., 1998; Becker and Shapiro, 2000, 2003; Levy and Berkowitz, 2003).

One possibility of dealing with non-Fickian transport is the continuous time random walk (CTRW) approach, a robust and easily applicable method introduced into hydrology by Berkowitz and Scher (1995). Examples of its application are: tracer migration in numerical simulations of fracture networks (Berkowitz and Scher, 1998), anomalous transport in a laboratory flow cell containing a heterogeneous porous media (Berkowitz et al., 2000) and a medium-scale field experiment in fractured till (Kosakowski et al., 2001).

In the following section, the experimental procedures will be described first, then the advection–dispersion model and the CTRW approach will be briefly introduced. Experimental results are analyzed using the model of Hadermann and Heer (1996) and the CTRW approach. Some reasons for the observed anomalous transport behavior of the colloids are then discussed.

2. CRR in situ experiments

The experiments analyzed in this paper were conducted in a shear zone at Nagra's Grimsel test site located in the crystalline rock of the Aar-massif in the Swiss Alps as part of the Colloid and Radionuclide Retardation (CRR) project. The shear zone was already utilized during former experiments (MI and EP).

Several boreholes were drilled from a tunnel into the planar experimental shear zone. Fig. 1 shows the intersection of the tunnel and the boreholes with the shear zone. For this study, only experiments in dipole #3, between the boreholes BOMI 08 and BOMI 10, are evaluated. For these experiments, borehole BOMI 10 was always used as a withdrawal well with an extraction rate Q_w of typically 150 ml min^{-1}. Borehole BOMI 08 was used for injection of the tracers with an injection flow rate Q_i of typically 10 ml min^{-1}. With the ratio $Q_w/Q_i = 15$, a full recovery of conservative tracers was achieved. The injection and the withdrawal boreholes are located 5 m from each other. For the injection, ground water from the experimental shear zone was collected before the experiment, stored under a cover gas (nitrogen) to minimize any possible changes in the water chemistry, and re-injected into the shear zone over the course of the experiments.

After the flow field had stabilized, one or more tracers were added to the injected water for 10 min in the form of a step input. Several different tracers were used during the tests

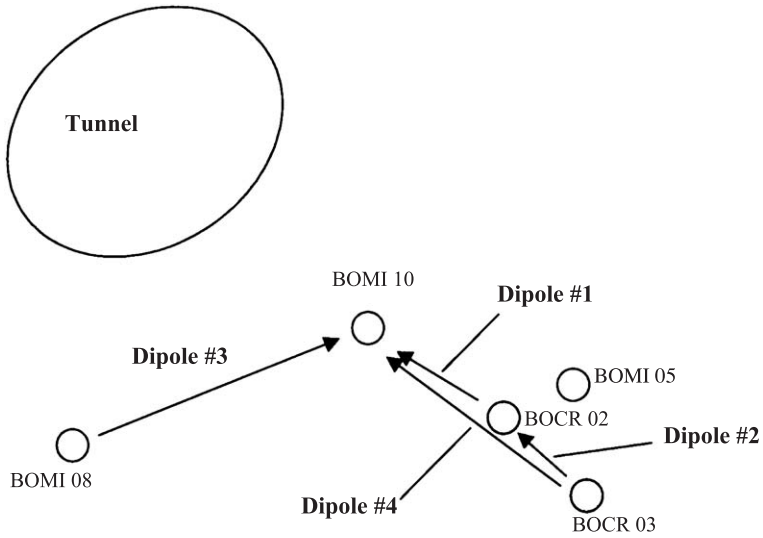

Fig. 1. Outline of the experiment: shown is the plane of the shear zone with the intersections of tunnel and boreholes. Only experiments in dipole #3 are evaluated in this paper. The distance between the boreholes in dipole #3, BOMI 08 (injection) and BOMI 10 (extraction) is 5 m.

conducted in this study. The measurements and the resulting breakthrough curves are summarized in the works of Möri (in press) and Hauser et al. (2002). The breakthrough curves for both, uranine and (bentonite) colloids are highly reproducible and the measurements are not biased by, e.g. temporal changes of the hydraulic boundary conditions. This study therefore concentrates only on the experimental runs #6 (uranine) and #6a (bentonite colloids). The breakthrough curves for colloids and uranine from these runs are shown in Fig. 2a.

To be able to compare the breakthrough of the different tracers, the concentrations of the solutes and colloids are normalized by division with the injected mass. If the colloid concentrations were measured as colloids per volume, the normalization was done with the injected number of colloids. The measured normalized colloid concentrations were scaled to a recovery of 100% in order to allow an easier comparison with the uranine measurements.

Uranine, which can generally be considered as a conservative (non-sorbing) tracer (see comments of Smith et al., 2001), was used as a reference for investigating the transport behavior. The migration behavior of uranine in this shear zone is well known from previous experiments (see, for example, Frick et al., 1992; Hadermann and Heer, 1996). Uranine concentrations using fluorometry were measured online at the end of the extraction flow line and in the injection borehole at the end of the injection line in order to monitor the injection function. Uranine recoveries are very high, usually more than 90%. An example for such an uranine breakthrough and the corresponding injection function is shown in Fig 2b. It is assumed throughout this study that all tracers have an injection function identical to the one measured for uranine.

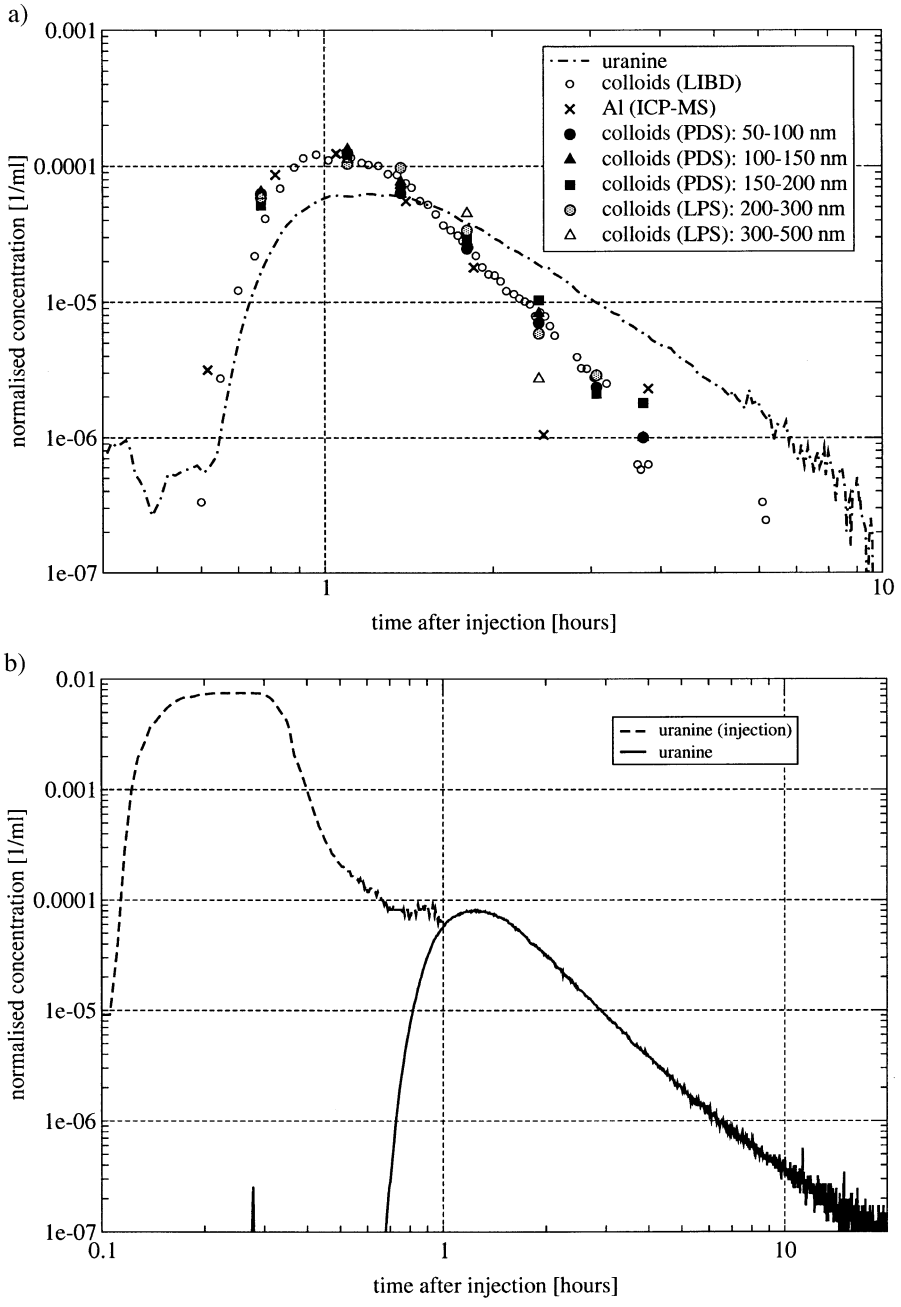

Fig. 2. (a) Breakthrough curves of colloids (run #6a) and uranine (run #6). (b) A typical uranine injection function and the corresponding breakthrough curve measured during run #16.

The uranine breakthrough curves in Fig. 2b shows the typical behavior normally associated with matrix diffusion (e.g. Tsang, 1995; Hadermann and Heer, 1996; Jakob, 1997), a slight retardation with respect to the colloids and an extensive tailing on the double-logarithmic scale.

A suspension of *bentonite colloids* with a concentration of about 20 mg l^{-1} was injected to evaluate the transport behavior of colloids in the shear zone. Water samples were taken for colloid concentration measurements (mass of colloids per unit fluid volume) using laser-induced breakdown detection (LIBD) (Hauser et al., 2002). The LIBD method integrates colloid numbers over all size classes, but measures predominantly small colloids. Additionally, the number of colloids per unit fluid volume in the different colloid size classes 50–100, 100–150, 150–200 nm was measured with a single particle monitor (PDS) and for the size ranges 200–300, 300–500, 500–700, 700–1000, 1000–1500, 1500–2000, 2000–5000 and over 5000 nm with a single particle spectrometer (LPS) (Degueldre et al., 1996b). Aluminum (Al) concentrations at the withdrawal well were measured with inductively coupled plasma mass spectrometry (ICP–MS). The injected bentonite colloids are the only tracer containing Al and, therefore, these measurements were used as additional method to detect the bentonite colloid breakthrough. The injected bentonite suspension was also investigated using PDS, LPS and ICPMS in order to measure the size distribution of the injected bentonite colloids for later comparison with the eluted colloid size distribution.

At the start of each experimental run, the concentration of *natural (background) colloids* in the groundwater of the experimental shear zone was determined with LIBD, PDS, LPS and Al. From previous investigations (see Degueldre et al., 1996a,b for an overview), it is already known that natural colloids occur in the groundwater in the experimental shear zone. The colloids consist mainly of amorphous silica with small amounts of mica and calcium silicates (Smith et al., 2001). It is not possible to differentiate directly between bentonite colloids and natural colloids with the utilized methods (LIBD, PDS, LPS and Al measurements). The measured concentrations are therefore a superposition of the concentrations of both colloid populations. Bentonite colloid concentrations are corrected by subtracting the natural colloid concentration from the measured concentrations.

The recoveries for the different colloid size classes, measured with PDS and LPS, decrease systematically with increasing size (see Table 1). PDS measurements for the smallest colloid size classes yield recoveries for the number of colloids of more than 90%,

Table 1
Colloid recoveries for run #6a

Tracer/detection method	Recovery
Colloids (LIBD)	55% (mass)
Al (ICP–MS)	50% (mass)
Colloid (PDS): 50–100 nm	90% (number)
Colloid (PDS): 100–150 nm	100% (number)
Colloid (PDS): 150–200 nm	100% (number)
Colloid (LPS): 200–300 nm	40% (number)
Colloid (LPS): 300–500 nm	16% (number)

whereas colloids in bigger size classes (not shown in Fig. 2a) yield very low recoveries. The mean mass recovery for the colloids measured with the LIBD method was about 55%. It is possible to estimate a rough value for the recovery of about 90% for the number of particles for the LIBD measurements with the help of the size distribution of the colloids (compare Section 5.3).

3. Models

In this study, two different models are used, which will be referred to as: (1) the 2D advection–dispersion (–matrix diffusion) model, and (2) the non-Fickian dispersion or CTRW (continuous time random walk) model.

(1) The first model is essentially the same as the model used by Hadermann and Heer (1996). Transport was considered to occur by advection and longitudinal dispersion in a fractures along 1D transport paths, retarded by diffusion into a porous rock matrix and sorption on rock matrix pore surfaces. Dispersion is modelled as a diffusion-like process, described by Fick's Laws (referred to as "Fickian dispersion" in the present study).

The 2D advection–dispersion model differs conceptually from the model of Hadermann and Heer only in its representation of the flow field and its inclusion of transverse dispersion. Additionally, it allows the inclusion of known artificial structures (e.g. tunnel) and more complicated regional boundary conditions (regional hydraulic gradients).

The advection–dispersion model explicitly includes matrix diffusion processes. It should be noted, that throughout this study, the term "advection–dispersion model" is used in preference to "advection–dispersion–matrix diffusion model".

(2) The non-Fickian dispersion or CTRW model provides a more generally applicable representation of advective and hydrodynamic dispersion processes in highly heterogeneous media. In this study, the CTRW model is used only for the interpretation of the experimental colloid breakthrough.

3.1. Advection–dispersion model

To date, nearly all attempts to model transport in the Grimsel shear zone have been based on a structural model described by Hadermann and Heer (1996), and this structural model is also used in the present work. Fig. 3 gives a sketch of the geological structure of the shear zone (upper part of the figure; note, this is already a simplification of reality), and the simplified conceptualisation for transport modelling (lower part). As in the work of Hadermann and Heer (1996), the complex and highly connected network of open and partially filled fractures observed in the actual shear zone is replaced by a set of parallel, open fractures, separated by a homogeneous porous rock matrix, representing the heterogeneous mixture of fault gouge, adjacent rock and dead end pores between the actual fractures. Transport in the simplified shear zone can be described by a single and constant (in time and space) set of material parameters. Based on the experience from previous experiments with similar dipole flow fields in the shear zone (summarized by Smith et al., 2001), it is reasonable to

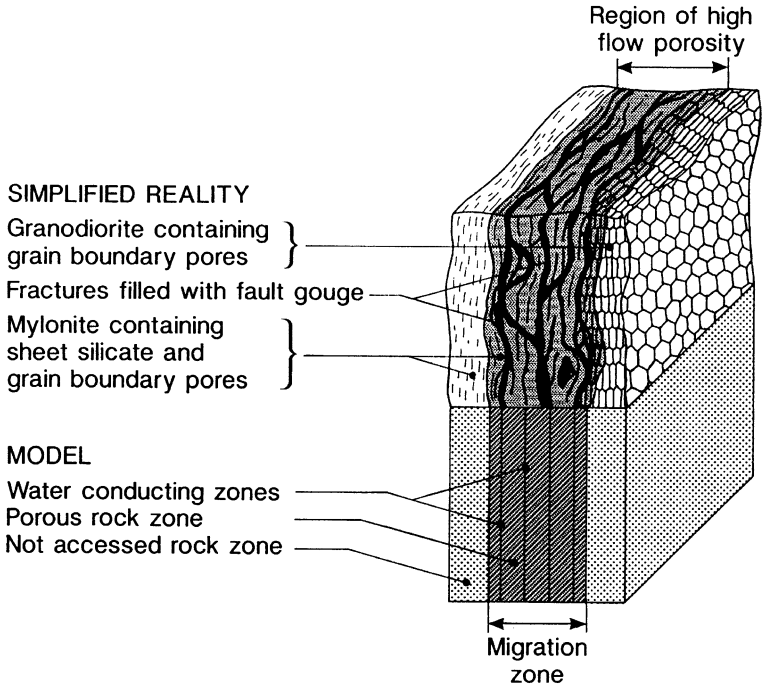

Fig. 3. Conceptual model of the shear zone (from Hadermann and Heer, 1996).

replace the shear zone by a single planar fracture with a uniform transmissivity. Solute is transported by advection and dispersion in the fractures and it can diffuse into the adjacent porous rock zone.

Transport is treated by using the advection–dispersion equation (Bear, 1972). Using this equation implies that the center of mass of the tracer plume moves with the mean fluid velocity and that the dispersion behaves macroscopically as a Fickian diffusion process, with the dispersivity being constant in space and time. It is assumed that the hydrodynamic dispersion coefficient D is linked to the mean fluid velocity $\bar{v}$ via a constant dispersivity (dispersion length): $D \sim \alpha\bar{v}$.

Streamlines in a dipole field are of varying length and tracer particles traveling along the streamline have different ''mean'' velocities. Thus, the shape of the breakthrough curve is mainly controlled by the travel times of tracers along different stream tubes and not by the dispersion in each stream tube.

The experiments evaluated in this study use withdrawal flow rates, which are 15 times higher than the injection flow rates. This results in a very asymmetric dipole with a near-radial convergent flow field. In such a flow field, the effect of streamline divergence is minimized. For the experiments analyzed in this study, it was even possible to achieve a reasonable fit with the Heer and Hadermann model utilizing only one 1D transport path (streamline). This is discussed more in detail in Section 5.2.

The governing equations for transport along a 1D transport path in a fractured porous medium are given, for example, by Heer and Hadermann (1996) and are not reproduced here. It is, however, also informative and useful for later discussions to consider some approximate solutions that illustrate the effects of matrix diffusion and sorption on the form of the breakthrough curves (see Hadermann and Heer, 1996).

The transport of a solute influenced by matrix diffusion along a streamline of the length L_i can be characterized by the peak-arrival time t_{mi}. The maximum of the breakthrough for a tracer reaches the outlet after

$$t_{mi} \approx \frac{L_i R_f}{\bar{v}_i} + \frac{2}{3}\tau_0 \tag{1}$$

$\bar{v}_i$ is the mean water velocity along a single streamline. The retardation factor R_f accounts for the retardation due to sorption on the fracture surfaces. The time shift accounting for matrix diffusion τ_0 is given by

$$\tau_0 = \left(\frac{\varepsilon_p}{b}\right)^2 \left(\frac{L_i}{\bar{v}_i}\right)^2 \frac{D_p R_p}{4} \tag{2}$$

ε_p is the porosity in the porous rock zone, D_p the pore diffusion coefficient in the porous rock, and R_p the retardation factor due to sorption in the porous rock.

The concentration C_{fi} at the fracture outlet after long times ($t \gg t_m$) is

$$C_{fi}(L_i, t) = \frac{M_0}{Q_w} \frac{\sqrt{\tau_0}}{\sqrt{\pi}} t^{-2/3} \tag{3}$$

M_0 is the (injected) total tracer mass and Q_w the extraction rate at the withdrawal well (observation point).

The effect of matrix diffusion and sorption in the porous matrix on the breakthrough of solutes is summarized in Fig. 4. This is an illustrative example only showing the key features of the breakthrough curves as predicted by the advection–dispersion model. The breakthrough curves were calculated for typical material parameters using the Picnic code (Barten, 1996). An initial solute pulse transported in the fracture by advection will be broadened by dispersion only as far as indicated by the solid black line. If matrix diffusion is a relevant process, the solute will be delayed and a typical tailing in the breakthrough curve, $C \sim t^{-3/2}$ (see Eq. (3) and compare also, e.g. Jakob, 1997) is observed. Sorption in the porous rock matrix will further delay the breakthrough.

3.2. Numerical implementation of the Fickian dispersion model

The modular software package RockFlow (Kolditz et al., 1999) was used for the transport calculations. RockFlow is based on the finite element method in a hybrid approach which enables the use of 1D, 2D and 3D elements in 3D space. The simulator uses an adaptive hierarchical grid, which re-adjusts itself during runtime based on multiple

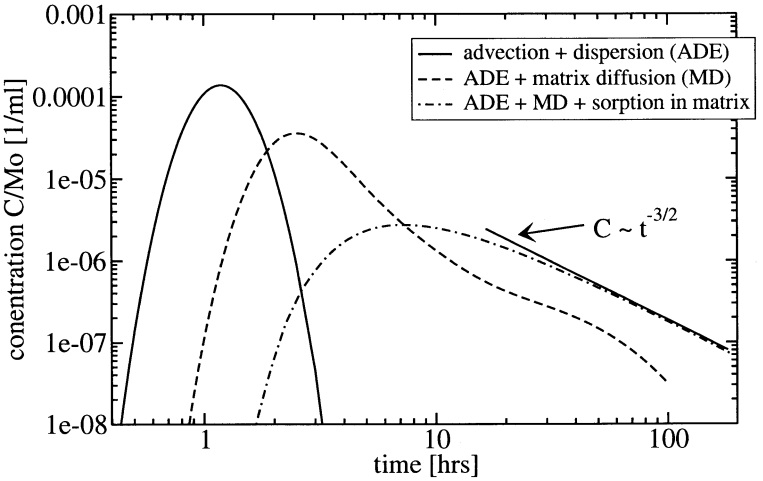

Fig. 4. Examples of the breakthrough curves produced by the advection and the dispersion of a solute in a fracture (solid line), the additional effect of limited matrix diffusion (dashed line) and sorption in the rock matrix (dashed–dotted line) on tracer breakthrough.

indicators. In this study, the RockFlow modules for fully saturated single-phase flow and reactive transport of one component is used.

A single fracture plane was constructed with 2D elements embedded in a matrix of 3D elements. Both flow and transport were calculated on the same grid. In a first step, the fluid velocity was calculated for the whole domain and transport was coupled to the flow via the fluid velocities in the elements. Fluid flow in a 2D element is calculated based on the so-called "cubic law", i.e. from the transmissivity of the element an equivalent "fracture aperture" can be calculated.

The transmissivity of the 2D elements was adjusted to the fracture aperture used and the hydraulic conductivity of the 3D elements was set to a very small value. In this way, fluid flow took place only in the 2D fracture elements. The dimensions of the model were 40×40 m. A constant head boundary condition was applied at the outer boundaries, and two nodes, spaced 5 m apart in the center of the model, were chosen as injection and withdrawal wells with constant fluid flow rates, as given by the experimental conditions. The chosen model dimensions and the boundary conditions ensure that the flow field between the wells, and in their vicinity, mimics the strongly asymmetric dipole field as closely as possible.

For transport calculations, a free outflow boundary condition (Neumann type boundary for which the diffusive flux is set to zero) was applied to the outer model boundaries. The large distance between the model boundaries and the injection/withdrawal points ensures that solutes do not reach the outer model boundaries. At the injection node, a time-dependent solute concentration was applied according to the experimentally measured uranine concentration in the injection well. Solute mass was removed at the extraction node according to the solute mass stored in the extracted fluid mass. At the start of the simulation, the solute concentration was set to zero in the whole domain. Transport

processes considered in the 2D fracture elements were advection and dispersion, and in the 3D matrix elements, diffusion.

3.3. Fitting procedure for the advection–dispersion model

The following procedure was applied for fitting the breakthrough curves and estimating the (material) parameters. The intention is to fit both colloid and uranine breakthrough curves with one consistent set of material parameters.

(1) Colloids are assumed to be excluded from matrix pores, and are thus not subject to the retardation processes of matrix diffusion and bulk sorption. Thus, to model colloid breakthrough, parameters associated with matrix diffusion and sorption can be set to zero, and breakthrough curves can be fitted by adjusting parameters associated only with advection and dispersion. The assumption that colloids are excluded from matrix pores is discussed more in detail in Section 5.3.

From Eq. (1), it is clear that for the colloids which are only transported in the fractures (no matrix diffusion), the tracer maximum comes after $t_m = L/\bar{v}$. Because the distance between the wells and the injection/withdrawal flow rates are fixed, the aperture of the fracture determines the magnitude of the velocity field and the mean flow velocity. In the case of multiple parallel fractures, the flow is distributed between all of the fractures and the fracture aperture is divided by the number of fractures. The fracture aperture is now fixed in such a way that the position of the maximum of the colloid breakthrough is reproduced.

The width of the measured breakthrough is fitted by adjusting the longitudinal dispersion length in the 2D model (in order to take into account the asymmetric dipole flow field). The transversal dispersion length was arbitrarily fixed at a value of 0.001 m. Earlier calculations with a very similar 2D model demonstrated that the calculated breakthrough curves are not sensitive to the value assigned to the transverse dispersion length (Smith et al., 2001).

(2) It is assumed that the parameters estimated from the breakthrough of the colloids are also applicable to conservative tracers retarded by matrix diffusion. Then, for a given dipole flow field, the breakthrough curves for these tracers can be fitted by adjusting parameters associated with matrix diffusion, but using the parameters associated with advection and dispersion that were obtained from the colloid breakthrough curves.

The effective matrix diffusivity, the product of porosity and pore diffusion coefficient can be extracted from Eq. (2), if assuming that uranine is non-sorbing. The other parameters in Eq. (2), b, L, $\bar{v}$ are already fixed from the modelling of the colloid breakthrough curve.

This fitting procedure combining fitting of the colloid and the uranine breakthrough curves assures a consistent set of material parameters and minimizes the number of free fitting parameters.

3.4. Continuous time random walk

The late time behavior displayed in the colloid breakthrough curves and their asymmetry are typical of non-Fickian transport. In the last few years, it has been

shown that a modelling approach based on continuous time random walk (CTRW) theory accounts very well for this type of transport. The formalism of the CTRW approach is well documented and summarized by Berkowitz et al. (2001), therefore, only the important points which are related directly to the following analysis are summarized.

Contaminant transport in varying velocity fields can be envisioned as particles moving through a geological formation via different paths with spatially changing velocities. Different paths are traversed by different numbers of particles. Typically, heterogeneous systems show a broader distribution of velocities than homogeneous ones. The velocity field in geological media is strongly correlated to the heterogeneity of the material. These heterogeneities can consist of fractures (joints and/or faults, connectivity of the system), variations in the rock matrix (i.e. grain sizes, mineralogy, layering, lithology and connectivity of the pores) and/or large-scale geological structures. The heterogeneities can occur on a broad scale of different spatial scales.

This kind of transport can be described in general by a joint probability density function, $\psi(s,t)$, which describes the probability for a particle displacement s, with a difference of arrival time, t. The idea is to map the important aspects of the particle motion in the fracture system onto $\psi(s,t)$. It can be shown that the principal characteristics of tracer movements are dominated by the behavior of $\psi(s,t)$ for a broad time range. Recent applications are restricted to advective transport of tracers, but it is also possible – at least in principle – to account for diffusive transport, as well as effects of adsorption/desorption. As discussed elsewhere, for example, by Berkowitz et al. (2001), non-Fickian transport arises in cases where the long time behavior of $\psi(s,t)$ is a power law, i.e. $\psi(s,t) \rightarrow t^{-1-\beta}$, with the constant exponent $\beta>0$. The relative shapes of the tracer transport curves, and the rate of the advance of the peak, vary strongly as a function of β. For $0<\beta<1$, transport is highly non-Fickian, and the concentration peak moves much more slowly than the average fluid velocity, with some particles advancing very fast. For $1<\beta<2$, the mean particle plume moves with the average fluid velocity (similar to the case of Fickian transport), but the particle distributions are more asymmetric than those of a Fickian distribution. For $\beta>2$, the transport becomes Fickian.

As in this study, tracer test measurements often consist of breakthrough curves of tracer concentrations as a function of time t, at selected distances from the tracer source. The tracer breakthrough usually refers to particles passing a sampling plane (and then exiting the system), and the (noncumulative) curve corresponds therefore to a first passage time distribution (FPTD). The FPTD is defined as the probability per time for a tracer particle to reach the site s for the first time. This concept is identical to the concept of a 1D advection–dispersion model (see also Section 5.2). The "injection" or source plane is the surface of the injection borehole and the exiting plane is essentially the surface of the extraction borehole. Transport between both planes (surfaces) is treated as one-dimensional. Dispersion in the measurement equipment is assumed negligible.

FPTD functions for different values of β are summarized by Berkowitz et al. (2001). The FPTD solutions for $0<\beta<1$ involves two explicit fitting parameters: β, which characterizes the dispersive process, and x_{shift}, which characterizes the effective tracer velocity at a given distance. In contrast, the FPTD solutions for $1<\beta<2$ requires three

fitting parameters: β, t_{mean} and b_β. A mean particle velocity can be calculated from the transport length, L, by dividing by t_{mean}. The case for $\beta=2$ is equivalent to the advection–dispersion equation and two fitting parameters are needed, namely t_{mean} and b_β. A mean particle velocity can be calculated from L by division with t_{mean}. It can be shown that, for the case $\beta=2$, b_β is directly related to the dispersivity D defined in the 1D advection–dispersion equation $b_\beta=D/L$ (Berkowitz et al., 2002).

As discussed by Kosakowski et al. (2001), convolution of the FPTD solutions can be used to deal with experimental systems in which either the input boundary condition is something other than a pulse or step input, or transport occurs through regions with distinctly different properties.

For the CTRW fits, the normalized measured uranine concentrations in the injection borehole were used and it was assumed that the injection functions for uranine and for the colloids are identical. The measured colloid breakthrough curves were fitted by performing a convolution between the injection solutions and the FPTD solutions. A combination of automated nonlinear curve fitting and manual selection of fitting parameters was used following Berkowitz et al. (2001).

CTRW fits of the uranine breakthrough are neither presented, nor used in this study. Though it is possible to achieve reasonable fits of the uranine breakthroughs with the basic CTRW approach, it is not clear how the fitting parameters are related to measurable parameters of, e.g. matrix diffusion. It is currently under investigation, which is the best way to treat processes like matrix diffusion or sorption in the framework of the CTRW approach.

4. Analysis of the tracer test data

In this section, first the fits of the colloid and the uranine breakthrough with the advection–dispersion model are presented. The idea was to do a combined fit of colloid and uranine breakthrough with a consistent set of material parameters for the 2D advection–dispersion model as described in Section 3.3.

In the last subsection, the fit of the colloid breakthrough with the alternative CTRW approach is provided.

4.1. Analysis of the colloid breakthrough with the advection–dispersion model

A fit of the normalized colloid breakthrough curves with the advection–dispersion approach is shown in Fig. 5. A velocity field based on four parallel fractures, each with an aperture of $2b=0.275\cdot10^{-4}$ m matched the observed maximum colloid breakthrough. Results from structural geology imply that the shear zone can be replaced by four parallel fractures (see Hadermann and Heer, 1996; Smith et al., 2001). It was either possible to match the early time behavior or the late time behavior of the colloidal breakthrough. The early time behavior and the height of the breakthrough maximum were matched by setting the longitudinal dispersion length to $5.0\cdot10^{-2}$ m. It should be stressed that it is not possible to reproduce the whole curve with a transport model based on the advection–dispersion approach without assuming physically unrealistic parameter values. The fit can

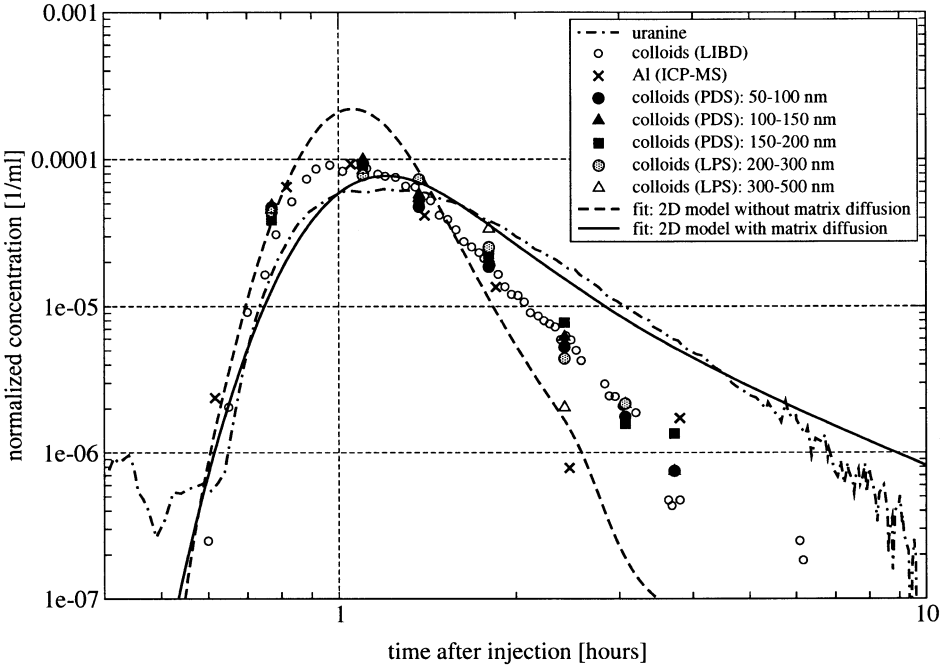

Fig. 5. Combined fit of the uranine and the colloid breakthrough with the advection–dispersion model.

be improved to match the late time behavior by assuming a (much) greater transversal dispersion length similar to or greater than the longitudinal dispersion length. This enlarges the spatial extent of the tracer plume and drives a part of the tracer into the outer regions of the dipole field where slower fluid velocities are encountered. This approach contradicts the findings in the Excavation Project, i.e. transport is limited to a relatively small zone of less than 0.5 m in width for a similar tracer test in the same shear zone (Möri, 2001).

4.2. Analysis of the uranine breakthrough with the advection–dispersion model

It is assumed that matrix diffusion alone is responsible for the delay of the uranine (compared to the colloids), therefore, the velocity field and the values for the dispersion lengths were taken from the fits of the colloid breakthrough. The uranine fit shown in Fig. 5 allows the calculation of the time shift τ_0 and, with help of Eq. (2), a combination of matrix porosity and pore diffusion coefficient was chosen, i.e. 0.075 for the porosity and $2.25 \cdot 10^{-11}$ m^2 s^{-1} for the pore diffusion coefficient. From Eq. (2), it is clear that different combinations of matrix porosity and pore diffusion coefficients can be used to generate the same fit. Without further information, it is not possible to select one specific combination of matrix porosity and pore diffusion coefficient. Hadermann and Heer (1996) included such information into their model and they estimated 0.062 ($+0.068$, -0.032) for the porosity and 2.5 ($+11$, -2) 10^{-11} m^2 s^{-1} for the pore diffusion coefficient.

In general, the advection–dispersion model with matrix diffusion provides a good fit to the uranine breakthrough curves, confirming in principle the findings of the earlier MI modelling studies.

Two remarks need to be added. First, the late time drop of the experimental breakthrough curve is probably an experimental artefact. Very low concentrations (below $1.0 \cdot 10^{-6}$ ml^{-1} in Fig. 5) should not be interpreted, because the measured values are highly biased and the concentration drop is not reproducible.

Second, it is not possible to achieve an exact match of the slope for the late time tails with the advection–dispersion model, not even with a model where matrix diffusion is limited to a porous matrix of finite thickness. All uranine breakthrough curves show a nearly constant slope of between -1.75 and -1.8 for the late time tail when plotted on logarithmic axes. The advection–dispersion model converges to curves with an exponent of -1.5 (compare also Fig. 4) for unlimited matrix diffusion.

Combining both observations, the problems in fitting the colloid breakthrough and in matching exactly the slope of the uranine tailing, it seems that the observed tailing in the uranine breakthrough is not only caused by matrix diffusion. In Section 5, several further possible causes for anomalous tailing in the breakthrough of colloids and solutes are compared, and it will be suggested that non-Fickian dispersion is also contributing to high late time concentrations of solute breakthrough in the shear zone.

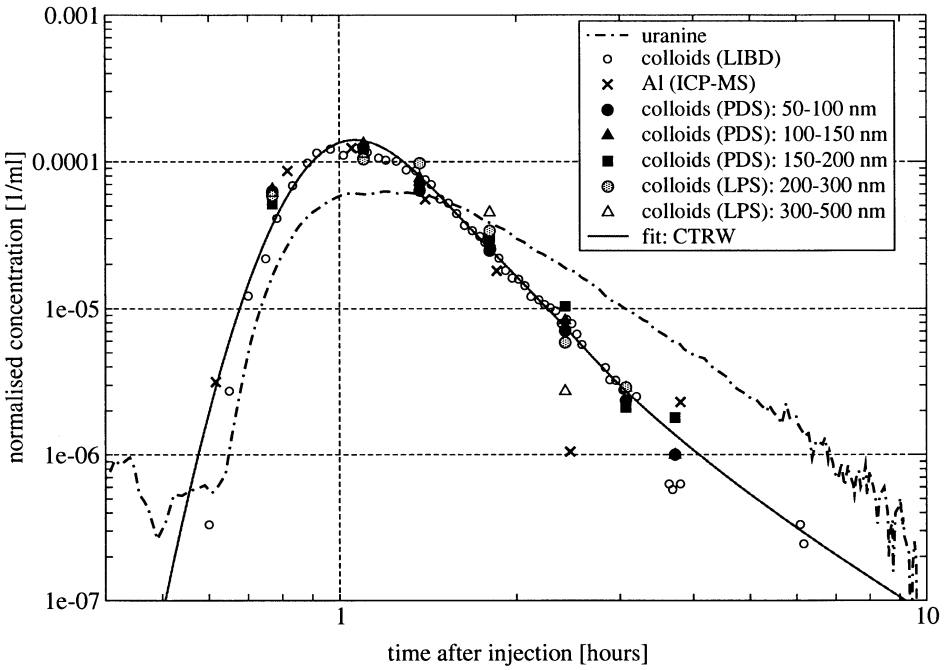

Fig. 6. CTRW-fit of the colloid breakthrough.

4.3. Analysis of the colloid breakthrough with the CTRW approach

Because of the difficulties of fitting the colloid breakthrough with the advection–dispersion model, an additional fit of the colloid breakthrough with the CTRW approach was carried out.

It was found that $\beta = 1.2$, $t_{mean} = 1.42$ [h] and $b_\beta = 0.28$ gives an optimal fit of the measured breakthrough curve as shown in Fig. 6. A mean particle (colloid) velocity of $9.8 \cdot 10^{-4}$ m s^{-1} can be calculated as described in Section 3.4.

The mean fluid velocity of the CTRW fit is lower than the one from the advection–dispersion fit, because the advection–dispersion approach matches the velocity for the breakthrough peak, whereas the CTRW approach yields the velocity of the center of mass of the colloid plume.

5. Connections between microstructure and transport behavior

A number of explanations have been proposed for the tailing of solute and colloid breakthrough curves in fractured geological media (Becker and Shapiro, 2000). This section considers whether the observed breakthrough tailing for the tests in the Grimsel shear zone is caused by (1) an artifact of the tracer injection process, (2) fractional breakthrough of streamlines due to the form of the flow field, (3) diffusive exchange of tracer with the rock, (4) diffusive exchange of tracer with stagnant water in the shear zone, (5) interaction of colloids with the fracture walls, or (6) advective and hydrodynamic processes.

5.1. Influence of the injection process

Often during tracer tests, the tracer is not injected as an ideal step function, but rather introduced with a significant tailing already. In such a case, the observed breakthrough will reflect this experimental artifact. The injection device used for the CRR tracer tests is equipped with a sensor for measuring the uranine concentration in the injection borehole. A typical injection function is shown in Fig. 2b. Sensitivity calculations with the CTRW solutions and the conventional advection–dispersion approach revealed that the tailing due to the measured injection function cannot explain the observed anomalies.

5.2. Fractional breakthrough of streamlines

In Section 3.1, it was already mentioned that the streamline divergence in the utilized asymmetric dipole flow field is minimized. This results in a small extension of the main transport path.

Additional support for a relatively small transversal extension of the main transport path comes from the fact that it was found possible to approximate the 2D advection–dispersion solution by a 1D advection–dispersion solution. The same fitting procedure as for the 2D advection–dispersion was used (see Section 3.3), i.e. the parameters estimated

from the breakthrough of the colloids (mean fluid velocity and dispersion length) are also used to fit the uranine breakthrough.

The mean fluid velocity was estimated to be $1.62 \cdot 10^{-4}$ m s^{-1} by matching the peak of the colloid breakthrough. It was found that a longitudinal dispersion length of 2.5 times greater than the one in the 2D model was needed to compensate for the effect of the dipole flow field and the non-consideration of transversal dispersion. The fitting parameters for the matrix diffusion are the same for the 1D and the 2D model.

Neither solution 1D nor 2D is able to fit both the early and the late time behavior of the colloid breakthrough. This finding provides also additional motivation for trying to evaluate the colloid transport with the CTRW approach, which is based on transport in a 1D flow field.

Additional evidence for a relatively small spreading of the tracers comes from the results of the Excavation Project. Tracer tests were conducted in the same shear zone only a few meters away from the current investigations. After completion of the tracer experiments, resin was injected and parts of the shear zone were excavated. The cores were analyzed and it was found that 90% of the retarded radionuclides could be excavated and a transport path with a maximum width of about 0.5 m could be identified (Möri, 2001).

5.3. Influence of diffusive processes on the transport

The size distribution of the bentonite colloids injected during the experiments roughly follows a power law with an exponent of -4 for the measured colloid sizes between 50 and 4000 nm:

$$\log(N) = 11.8 - 4\log(2r)$$

where N is the number of colloids per milliliter and r is the radius of the colloids. The size distribution of the natural Grimsel groundwater colloids is very similar:

$$\log(N) = 14.5 - 4\log(2r)$$

(see also Degueldre et al., 1990).

The diffusivity coefficient D_0 for colloids in free water depends on temperature T, dynamic viscosity μ of the water, the Boltzmann constant $k_B = 1.38 \times 10^{-23}$ J/kg and the radius r of the spherical colloids. D_0 can be calculated using the Stokes–Einstein equation: $D_0 = (k_B T)/(6\pi\mu r)$. That is, for a colloid diameter of 75 nm, the diffusivity coefficient in water is $1.7 \cdot 10^{-13}$ m^2 s^{-1} and for a colloid diameter of 400 nm only $0.3 \cdot 10^{13}$ m^2 s^{-1}. In a porous medium, the effective diffusivity depends on the structure of the pore space: porosity, tortuosity (accounting for the tortuous path of real pores), and constrictivity (accounting for the fact that the cross-section of a pore segment varies over its length). The effective diffusion coefficient in a porous medium is lower than the diffusion coefficient in free water by a factor of multiplication between 0.01 (clay) and 0.7 (sands) (de Marsily, 1986). Therefore, it can be concluded that the effective matrix diffusion coefficient for the smallest measured colloid size class is below $1.7 \cdot 10^{-13}$ m^2 s^{-1}.

James and Chrysikopoulos (1999) have investigated the influence of matrix diffusion on the breakthrough of polydispersed colloids in rough fractures. They could show that larger colloids are least retarded and smaller colloids are more slowly transported.

Although it is possible to fit the breakthrough curve of the colloids with a matrix-diffusion model, it is not possible to find a reasonable combination of matrix porosity, fracture aperture and diffusion coefficient. The fit in Fig. 7 is based on a pore diffusion coefficient of $1.0 \cdot 10^{-11}$ m^2 s^{-1}, i.e. at least 50 times greater than the diffusion coefficient in water for colloids of 75-nm diameter.

The normalized colloid breakthrough curve in Fig. 7 is independent of the colloid size. If matrix diffusion or diffusion into stagnant water zones are responsible for the tailing, the peak arrival times (and the slope of the early tail) should change with the diffusivity of the transported substance according to Eqs. (1) and (2). The smallest colloids, with a mean size of 75 nm, are about five times smaller than the biggest colloids (mean size 400 nm). Changing the diffusivity by a factor of 5, as for the dashed line in Fig. 7, results in a clear shift of the breakthrough curve. Such a shift was not observed in the measured breakthrough curves and it can be concluded that diffusive processes, such as matrix diffusion or diffusion into zones of stagnant water, have only a minor influence on the transport of colloids in the shear zone.

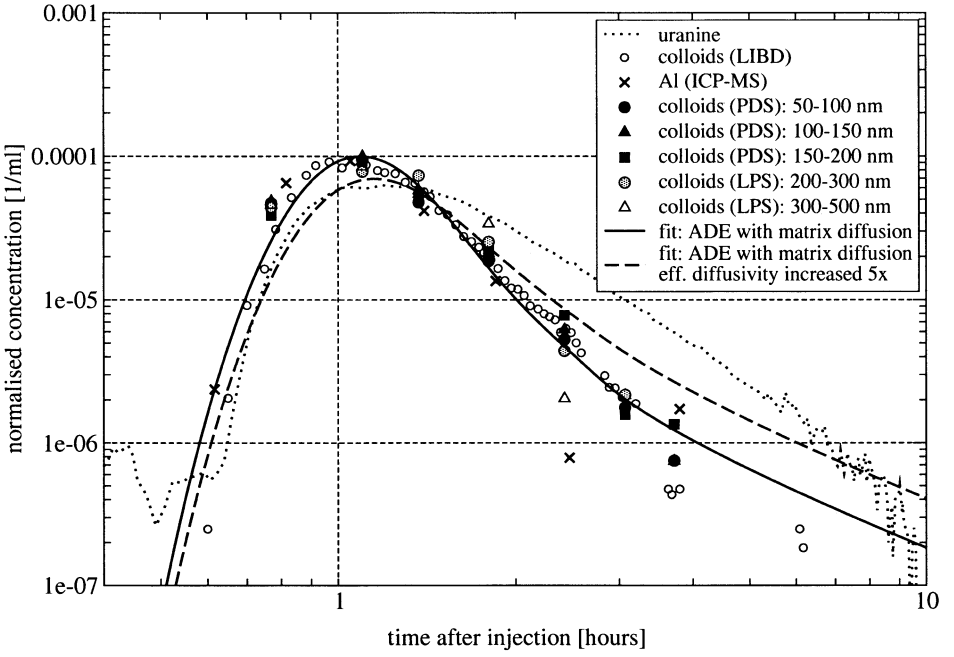

Fig. 7. Two fits for colloid breakthrough with an advection–dispersion (matrix diffusion) model to investigate the influence of the colloid size on the transport. The second curve was calculated for a five times higher pore diffusion coefficient, which corresponds to a five times smaller colloid size.

5.4. Interaction of colloids and fracture walls

Colloids are mobile in the fluid phase, but their transport may be retarded by interaction with the fracture surface. They can become immobilized by mechanical filtration, sedimentation (gravitational settling) at the bottom of a fracture, and electrochemical filtration such as electrostatic attraction or chemical adsorption. It is commonly assumed that colloid deposition takes place in two rate-limiting steps. The first step is the transport of colloids to fracture surfaces by Brownian motion, interception, or gravitational settling, resulting in collisions of the colloids with the fracture surface. The second step is the attachment of the colloids to the surface due to interparticle forces between colloids and fracture surface.

James and Chrysikopoulos (1999, 2000) showed that for the case of kinetic deposition at fracture surfaces, the smallest colloids are preferentially deposited onto the fracture walls and that colloid distributions are discretized according to colloid size (additional to the effect of matrix diffusion already discussed in the previous Section 5.3). Again, the peak of the measured breakthrough curves does not shift in time with the colloid size, nor does the measured late time tailing show any dependence on the colloid size. These findings contradict any major contribution of deposition mechanisms since a dependence on colloid size would be expected.

An additional argument for negligible interactions between colloids and fracture surfaces is the high pH-value of the Grimsel groundwater (pH~9.6). For such a high pH-value, the bentonite colloids, as well as the natural groundwater colloids and the rock surface, possess a negative surface charge and the attachment of colloids to the rock surface is weak (Degueldre et al., 1996a,b). The short mean residence time of the bentonite colloids in the shear zone due to the high fluid velocities during the tracer tests also minimizes the probability of an interaction between colloids and fracture surfaces.

The measurements of colloid breakthrough show a complete recovery, in terms of colloid numbers, for colloid sizes smaller than 200 nm, about 40% for colloids between 200 and 300 nm and 16% for a colloid size of 300–500 nm (Table 1). Gravitational settling and/or mechanical filtration are both possible mechanisms explaining this observation. Both processes are not predominantly governed by the diffusivity of the colloids. Therefore, gravitational settling and mechanical filtration do not contradict the finding that diffusive processes have only minor influence on the observed tailing in the colloid breakthrough curve.

5.5. Influence of the flow field on the transport

It was observed in previous experimental studies that advective processes can cause non-Fickian spreading of colloids and anomalous tailing of breakthrough curves for solutes and colloids (e.g. Hatano and Hatano, 1998; Sidle et al., 1998; Becker and Shapiro, 2000). A general, physically based approach to quantify non-Fickian transport is based on the CTRW method described in Section 3.4. Berkowitz and Scher (1998) conducted numerical experiments for particle transport in 2D fracture networks. They could show that the dominant aspects of particle transport in fracture networks—non-Fickian transport—results from subtle features of the steady flow-field distribution through the network

and that there is a quantitative agreement between their simulations and the CTRW approach. Park et al. (2003) extended this approach to the investigation of particle transport at 3D fracture intersections. Transport simulations at fracture intersections showed that local flow circulations can arise from variability within the hydraulic head distribution along fracture intersections and from the internal no flow condition along fracture boundaries. They found that local flow cells might act as an effective mechanism to enhance the long breakthrough tailing in discrete fracture networks, but have little effect on the overall fluid flow in a fracture network.

As shown by Hoehn et al. (1990) and Meier et al. (2001), the transmissivity distribution in the Grimsel shear zone is rather heterogeneous. The undisturbed flow field can be rather complex and flow along preferential paths is a dominant process. They also noted that characterizing a transmissivity field based on hydraulic information alone does not necessarily lead to successful transport predictions.

The Excavation Experiment (EP), as summarized already in the introduction, focused on the detailed investigation of the shear zone structure. Although it was known that the shear zone is highly heterogeneous, the main result was that open channels in the shear zone control the radionuclide migration to a very high degree (Fig. 8). Radionuclides were found in dead-end channels, short-cuts between adjacent channels and merging and bifurcations of pathways occurred on the meter and centimeter scale.

By comparing the findings of the EP project (Möri, in press) with the numerical investigations of Berkowitz and Scher (1998), it can be inferred that the occurrence of an interconnected network of flow channels in conjunction with low velocity regions (e.g. in ‘‘dead-end’’ fractures) is one possible reason for the observed late time tailing for the colloids. In natural fracture networks, dead-end fractures are not ‘‘dead’’ in terms of fluid flow. Small pressure differences will set up local flow cells and particles can advectively enter such flow cells and will be delayed compared to particles not entering such low velocity zones. In general, the occurrence of low velocity regions will cause a delay of some particles. From structural geological investigations, it is known that the flow channels are partially filled with non-cohesive fault gouge material. This material is highly porous and can permit water flow (Smith et al., 2001; Möri, in press). It can be expected that the fluid velocities and therefore the particle velocities are higher in the open channels than in the filled parts of the fracture. Particles entering the filled fractures will be delayed.

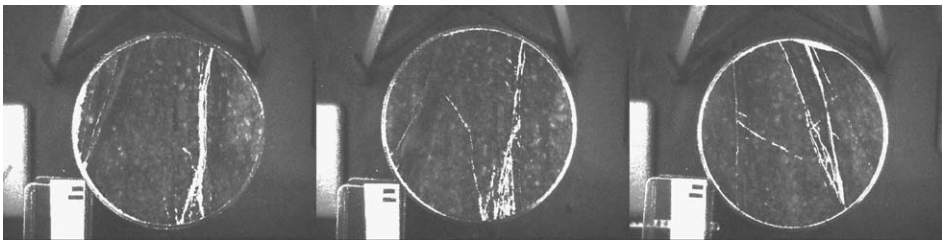

Fig. 8. Example for flow channels in cores recovered during the EP experiment. The radius of the rock is 0.15 m. With resin impregnated flow channels are clearly visible under UV light. Left: channel type structure, middle: braided type structure, right: network type structure (photos adapted from Möri, 2001).

Transport processes in the open parts of the shear zone will differ completely from the ones in the fault gouge filled parts (Lunati et al., 2003). In the fault gouge filled parts, the transport behavior is much smoother and contaminant fronts move much more regularly than in open rough fractures.

This mechanism will also affect the transport of solutes. In the case of solutes, there are at least two possible mechanisms causing retardation and breakthrough tailing, namely, matrix diffusion and advective transport in a small-scale fracture network and low velocity zones. Fitting the breakthrough curves of a conservative tracer, without considering the influence of the nature of the flow field, leads to an overestimation of the matrix diffusion.

Additionally, the effective fracture surface available for matrix diffusion might be underestimated. In a fracture network, the available surface is much larger than in a set of parallel fractures with the same hydraulic transmissivity. In local flow cells, the fluid velocity is smaller and the solute entering such slow velocity zones has more time to diffuse into the matrix.

All of these effects have to be compensated by an appropriate choice of values for the fitting parameters in an advection–dispersion model utilizing the parallel plate representation of a fracture. Anomalous transport due to fracture network effects and slow velocity regions, different time constants for matrix diffusion in slow velocity regions, and a possible underestimation of the available surface area are then compensated by a change of the fracture aperture/effective surface area, fluid velocity, matrix porosity and pore diffusion coefficient in the matrix.

6. Summary and outlook

The colloid breakthrough curves analyzed in this study display behavior that is characteristic of non-Fickian transport. The conventional models based on matrix diffusion and a Fickian representation of the dispersion process clearly fail to describe and explain the measured breakthrough curves. This data set was analyzed with a CTRW approach, which allows a connection between a physical-based picture of colloid (particle) motion with the geometric and hydraulic characterization of the shear zone.

The experimental data and theoretical considerations presented in this paper give strong indications that advective transport processes, closely connected to the microstructure of the Grimsel shear zone, are responsible for the observed anomalous tailing of the colloid breakthrough. It seems unlikely that diffusive processes, fractional breakthrough of individual streamlines, experimental artifacts (e.g. injection function) or the interaction of colloids with the fracture walls have any significant influence on the transport.

This study shows that it is possible to fit the breakthrough curves of conservative tracers successfully utilizing the advection–dispersion–matrix diffusion conceptual model developed during MI. However, if non-Fickian dispersion is of relevance, the tailing in the breakthrough of solutes is caused by a complex interaction of advective processes and diffusion into the porous material, which surrounds the open fractures. Parameters for safety assessment derived by fitting tracer transport experiments using advection–

dispersion (-matrix diffusion) models based on Fickian dispersion need to be viewed with caution.

In the methodology for applying the advection–dispersion model, it is assumed that advection and dispersion parameters will be identical for solutes and for colloids. When colloid attachment to surfaces is not favored, more rapid transport of colloids compared to molecular tracers is expected based on their size and their reduced Brownian diffusivity (see, e.g. Section 10.2.4 in de Marsily, 1986). If colloids have the same charge as the wall material of the fractures, repulsion effects tend to move colloids more to the center of the fracture where water velocities are higher. This causes the average colloid velocities to be larger than the average water velocity. Hydrodynamic chromatography and size-exclusion chromatography are established laboratory methods that elute the largest macromolecule first and molecular tracers last.

These kinds of velocity enhancements are subtle, however, and are expected to be smaller than the retardation effects due to matrix diffusion. Hydrodynamic chromatography, the retardation of colloids according to their size, could not be observed. The influence of such effects on the colloid transport cannot be ruled out, but it is also not possible to quantify them with the available experimental data. Some colloids were, however, filtered during transport. The dependence of the degree of filtration on colloid size suggests that gravitational settling and/or mechanical filtration are the most likely immobilisation mechanisms.

The models applied to modelling the CRR in situ tests are highly simplified, and may only be applicable, or ''valid'', over the spatial and temporal scales of the CRR experiments. The modelling approach used in the present study may therefore not be directly applicable to safety assessment problems and the direct implications of the results of this study for safety assessment are limited. It can, however, be said that the study has demonstrated the high degree of mobility of bentonite and other colloids in a system that is at least in some ways comparable to those of interest in safety assessment.

Acknowledgements

I would like to thank Russell Alexander, Mike Bradbury, Jörg Hadermann, Andreas Jakob, and Ralph Mettier for their helpful comments on the manuscript. Special thanks go to Brian Berkowitz and Paul Smith for their numerous helpful comments and suggestions.

Thanks to Res Möri, Horst Geckeis, Thomas Fierz and Claude Degueldre for the help with the experimental data. Results were provided in the framework of the Colloid and Radionuclide Retardation project, (which is conducted in the frame of Phase V at the Grimsel Test Site) and the funding partners, namely Nagra (Switzerland), ENRESA (Spain), ANDRA (France), JNC (Japan), USDOE/SNL (USA) and FZK-INE (Germany), are gratefully acknowledged.

This work was partially financed by the National Cooperative for the Disposal of Radioactive Waste (Nagra).

References

Barten, W., 1996. Linear response concept combining advection and limited rock matrix diffusion in a fracture network transport model. Water Resour. Res. 32 (11), 3285–3296.

Bear, J., 1972. Dynamics of Fluids in Porous Media Elsevier, New York.

Becker, M.W., Shapiro, A.M., 2000. Tracer transport in fractured crystalline rock: evidence of nondiffusive breakthrough tailing. Water Resour. Res. 36 (7), 1677–1686.

Becker, M.W., Shapiro, A.M., 2003. Interpreting tracer breakthrough tailing from different forced-gradient tracer experiment configurations in fractured bedrock. Water Resour. Res. 39 (1), 1024 (doi:10.1029/2001WR001190).

Berkowitz, B., Scher, H., 1995. On characterization of anomalous dispersion in porous and fractured media. Water Resour. Res. 31 (6), 1461–1466.

Berkowitz, B., Scher, H., 1998. Theory of anomalous chemical transport in fracture networks. Phys. Rev., E Stat. Phys. Plasmas Fluids Relat. Interdiscip. Topics 57 (5), 5858–5869.

Berkowitz, B., Scher, H., Silliman, S.E., 2000. Anomalous transport in laboratory-scale, heterogeneous porous media. Water Resour. Res. 36 (1), 149–158 (with a minor correction, published in Water Resour. Res., 36 (5) 1371).

Berkowitz, B., Kosakowski, G., Margolin, G., Scher, H., 2001. Application of continuous time random walk theory to tracer test measurements in fractured and heterogeneous porous media. Ground Water 39 (4), 593–604.

Berkowitz, B., Klafter, J., Metzler, R., Scher, H., 2002. Physical pictures of transport in heterogeneous media: advection–dispersion, random walk and fractional derivative formulations. Water Resour. Res. 38 (10), 1191 (doi:10.1029/2001WR001030).

Degueldre, C., Longworth, G., Moulin, V., Vilks, P., Ross, C., Bidoglio, G., Cremers, A., Kim, J., Pieri, J., Ramsay, J., Salbu, B., Vuorinen, U., 1990. Grimsel test site—Grimsel colloid exercises: an international intercomparison exercise on the sampling and characterization of groundwater colloids. Nagra Tech. Report NTB 90-01, National Cooperative for the Disposal of Radioactive Waste, Wettingen, Switzerland.

Degueldre, C., Grauer, R., Laube, A., Oess, A., Silby, H., 1996a. Colloid properties in granitic groundwater systems: II. Stability and transport study. Appl. Geochem. 11, 697–710.

Degueldre, C., Pfeiffer, H.-R., Alexander, W., Wernli, B., Brütsch, R., 1996b. Colloid properties in granittic groundwater systems: I. Sampling and characterization. Appl. Geochem. 11, 677–695.

de Marsily, G., 1986. Quantitative Hydrogeology: Groundwater Hydrology For Engineers Academic Press, New York.

Frick, U., Alexander, W.R., Baeyens, B., Bossart, P., Bradbury, M.H., Bühler, Ch., Eikenberg, J., Fierz, Th., Heer, W., Hoehn, E., McKinley, I.G., Smith, A., 1992. Grimsel test site—The radionuclide migration experiment: overview of investigations 1985–1990. Nagra Tech. Report NTB 91-04, National Cooperative for the Disposal of Radioactive Waste, Wettingen, Switzerland.

Hadermann, J., Heer, W., 1996. The Grimsel (Switzerland) migration experiment: integrating field experiments, laboratory investigations and modelling. J. Contam. Hydrol. 21, 87–100.

Hatano, Y., Hatano, N., 1998. Dispersive transport of ions in column experiments: an explanation of long-tailed profiles. Water Resour. Res. 34 (5), 1027–1033.

Hauser, W., Geckeis, H., Kim, J.I., Fierz, Th., 2002. A mobile laser-induced breakdown detection system and its application for the in situ-monitoring of colloid migration. Colloids Surf., A Physicochem. Eng. Asp. 203, 37–45.

Heer, W., Hadermann, J., 1996. Modelling radionuclide migration field experiments. PSI Report 91-13, Paul Scherrer Institut, Villigen, Switzerland.

Hoehn, E., Fierz, Th., Thorne, P., 1990. Grimsel test site—Hydrogeological characterization of the migration experimental area. PSI Report 60, Paul Scherrer Institut, Würenlingen and Villigen, Switzerland.

Jakob, A., 1997. Modelling solute transport using the double porous medium approach. In: Grenthe, I., Puigdomenech, I. (Eds.), Modelling in Aquatic Chemistry. OECS/NEA, Paris, France.

James, S.C., Chrysikopoulos, C.V., 1999. Transport of polydisperse colloid suspensions in a single fracture. Water Resour. Res. 35 (3), 707–718.

James, S.C., Chrysikopoulos, C.V., 2000. Transport of polydisperse colloids in a saturated fracture with spatially variable aperture. Water Resour. Res. 36 (6), 1457–1465.

Kolditz, O., Kaiser, R., Habbar, D., Rother, T., Thorenz, C., 1999. ROCKFLOW—Theory and Users Manual, Release 3.4, Groundwater Modelling Group, Institute of Fluid Mechanics, University of Hannover.

Kosakowski, G., Berkowitz, B., Scher, H., 2001. Analysis of field observations of tracer transport in a fractured till. J. Contam. Hydrol. 47 (1), 29–51.

Levy, M., Berkowitz, B., 2003. Measurement and analysis of non-Fickian dispersion in heterogeneous porous media. J. Contam. Hydrol. 64 (3–4), 203–226 (doi:10.1016/S0169-7722(02)00204-8).

Lunati, I., Kinzelbach, W., Sørensen, I., 2003. Effects of pore volume-transmissivity correlation on transport phenomena. J. Contam. Hydrol. 67 (1–4), 195–217 (doi:10.1016/S0169-7722(03)00065-2).

McKinley, I.G., Alexander, W.R., Bajo, C., Frick, U., Hadermann, J., Herzog, F.A., Hoehn, E., 1988. The radionuclide migration experiment at the Grimsel Rock Laboratory, Switzerland. Sci. Basis Nucl. Waste Manage. XI, 179–187.

Meier, P.M., Medina, A., Carrera, J., 2001. Geostatistical inversion of cross-hole pumping tests for identifying preferential flow channels within a shear zone. Ground Water 39 (1), 10–17.

Möri, A., 2001. Radionuclide Retardation Project at the GTS—an overview of lessons learned and ongoing experiments, in first TRUE stage—transport of solutes in an interpreted single fracture, Proceedings from the 4th International Seminar Äspö, September 9–11, 2000, SKB Tech. Report TR-01-24, 181–202, Swedish Nuclear Fuel and Waste Management, Stockholm, Sweden, 2001.

Möri, A., (Ed) 2003. The CRR final project report series: 1. Description of the field phase—methodologies and raw data. Nagra Technical Report NTB 03-01, Nagra, Wettingen, Switzerland (in press).

Ota, K., Alexander, W.R., Smith, P.A., Möri, A., Frieg, B., Frick, U., Umeki, H., Amano, K., Cowper, M.M., Berry, J.A., 2002. Building confidence in radionuclide transport models for fractured Rock: the Nagra/JNC radionuclide retardation programme. Mater. Res. Soc. Symp. Proc. 633, 1033–1041.

Park, Y.-J., Lee, K.-K., Kosakowski, G., Berkowitz, B., 2003. Transport behavior in three-dimensional fracture intersections. Water Resour. Res. 39 (8), 1215 (doi:10.1029/2002WR001801).

Sidle, C.R., Nilsson, B., Hansen, M., Fredericia, J., 1998. Spatially varying hydraulic and solute transport characteristics of a fractured till determined by field tracer tests, Funen, Denmark. Water Resour. Res. 34 (10), 2515–2527.

Smith, P. A., Alexander, W. R., Heer, W., Fierz, T. Meier, P. M., Baeyens, B., Bradbury, M. H., Mazurek, M., McKinley, I. G., 2001. The Nagra-JNC in situ study of safety relevant radionuclide retardation in fractured crystalline rock I: radionuclide migration experiment—overview 1990–1996. Nagra Tech. Report NTB 00-09, National Cooperative for the Disposal of Radioactive Waste, Wettingen, Switzerland.

Tsang, Y.W., 1995. Study of alternative tracer tests in characterizing transport in fractured rocks. Geophys. Res. Lett. 22 (11), 1421–1424.